Supporting Information

Size Structure - Catalytic Performance Correlation of Supported Ni/MCF-17 Catalysts for CO_x-free Hydrogen Production

Yanping Li, [a] Jie Wen, [a] Arshid M. Ali, [b] Ming Duan, [a] Wei Zhu, [c] Hui Zhang, *[a] Chen Chen [c] and Yadong Li [c]

[a] The Center of New Energy Materials and Technology, College of Chemistry and Chemical Engineering, Southwest Petroleum University, Chengdu 610500, China

[b] Department of Chemical & Materials Engineering, King Abdulaziz University, Jeddah 72523, Kingdom of Saudi Arabia

[c] Department of Chemistry, Tsinghua University, Beijing 100084, China

E-mail: huizhang@swpu.edu.cn

Table of Contents

1. Experimental Section

Synthesis of Ni-based catalysts

Synthesis of Ni nanoparticles. All reagents used in this work are of analytical grade. 0.12 g $Ni(acac)_2$, 0.16 mL oleic acid (OA) and 7.5 mL oleylamine (OAm) were mixed in a three-neck flask. Dissolution of $Ni(acac)_2$ at 60 ^oC was carried out under Argon flow and continuous magnetic stirring. Later, the temperature was raised to 110 ^oC and was kept for 1 h to remove dissolved oxygen and impurities, such as water. Soon after, 1 mL of OAm solution with 0.13 g Borane tert-butylamine complex (TBAB) was quickly injected into the above solution. A rapid color change from light green to black indicated nickel species reduction and the reaction was allowed to continue at 110 ^oC for 15 min. After centrifugation with ethanol, the final nickel nanoparticle were stored in 10 mL of hexane for further use. All above steps were repeated to reduce nickel species under different temperatures of 90 °C, 150 °C and 180 °C. Ni nanoparticles obtained under different reduction temperatures of 90 °C, 110 °C, 150 °C and 180 °C were denoted as NiR90, NiR110, NiR150 and NiR180.

In addition, following nickel nanoparticle were also prepared under similar method with slight modification:

i. 0.06NiR180: 0.06 g of $Ni(acac)_2$ instead of 0.12 g.
ii. NiR90 and NiR110: simultaneous addition of $Ni(acac)_2$ and TBAB to the flask at room temperature instead of elevated temperature to study the effect of reduction temperature on nickel particle size.
iii. Ni180: Same method but without TBAB.

Synthesis of support MCF-17. A solution, obtained after adding 4 g of triblock copolymer Pluronic P123 (BASF) dissolved in an acidic solution (10 mL of 37 wt% HCl and 65 mL of H_2O) to 4g of 1,3,5-trimethylbenzene (TMB), was heated to 37-40 °C under vigorous stirring for 2 h. Later, 9.2 mL of tetraethoxysilane (TEOS) was added and stirred for 5 min. The solution mixture was aged in autoclave at 40 °C for 20 h under a quiescent condition. Further, 46 mg of NH_4F was added to the mixture and again aged at 100 °C for another 24 h. The resulting precipitate was filtered and

multiple rinsed with water and ethanol, then dried. The obtained white powder MCF-17 was calcined in air at 900 °C for 6 h. In addition, both pore and window sizes of spherical MCF-17 was adjusted by varying TMB and NH_4F quantities, as well as the synthesis temperature.

Synthesis of supported Ni-based catalysts. Precise amounts of Ni nanoparticles dispersion was added to the solution that obtained by adding 0.98 g of spherical MCF-17 in. After 10 h of ultrasonic stirring, suspension was filtered, multiple rinse with hexane and dried in ceramic dish. Later, it was placed in a tube furnace with flow of Argon, and was heated to 400 ^oC with 2 ^oC/min temperature ramp for 5 h before it was cooled down to room temperature. The Ni nanoparticles supported on MCF-17 were collected and stored. All the catalysts were named as NiR90/MCF-17, NiR110/MCF-17, NiR150/MCF-17, NiR180/MCF-17, 0.06NiR180/MCF-17, NiCR90/MCF-17, NiCR110/MCF-17 and Ni180/MCF-17.

Characterizations

The X-ray diffraction (XRD) patterns of the samples were measured on an X'Pert PRO MPD diffractometer using a X'Celerator detector and Cu Kα radiation (λ = 1.5406 Å) operating at 40 kV and 40 mA from 10° to 80° with a 2θ step size of 0.02°. Transmission electron microscope (TEM) images were measured on a FEI Tecnai G2 F20 field emission transmission electron microscope with accelerating voltage of 200 kV. One drop of the suspension sample was added to a carbon-coated copper mesh for transmission electron microscope analysis. The specific surface areas, pore volumes, average pore sizes and pore size distributions of the catalysts were measured by N_2 adsorption-desorption on a Quadrasorb SI analyzer (Quantachrome, USA) at 77 K after degassing the samples for 3 h at 573 K. The surface areas, pore sizes and pore volumes obtained from N_2 adsorption-desorption measurement. Specifically, pore size D_{BJH} obtained from the maximal of the pore size distribution curve calculated by the BJH method, the pore volumes calculated from the desorption branch of N_2 physisorption isotherm. The X-ray photoelectron spectra (XPS) patterns were measured on a Thermo ESCALAB 250XI instrument using a monochromatic Al-Kα X-ray source under the conditions of 1486.6 eV. H_2 chemisorption were performed at

40 ^{o}C by using ChemBET Pulsar Automatic Chemisorption Analyzer (Quantachrome Instrument). A 200 mg catalyst sample was reduced at 400 ^{o}C with H_2 for 1 h. Then, the H_2 flow was replaced with Ar flow for 1 h to remove the residual H_2 and the temperature was decreased to 40 ^{o}C. Finally, Ni particle sizes and Ni dispersion were measured. A spherical model for the metal nanoparticles and H/Ni adsorption stoichiometry 1 is assumed in calculating the metal dispersion.

Catalytic measurements

The NH_3 decomposition reactions were performed in a fixed-bed quartz microreactor (about 4 mm i.d.) under atmospheric pressure, 6000 $mL \cdot g_{cat}^{-1} \cdot h^{-1}$ gas hourly space velocity (GHSV) and reaction temperature at 573–873 K. Prior to catalytic conversion of NH_3 measurement, the catalysts were reduced in a 5% H_2/Ar gas mixture (flow rate of 30 mL/min) at 673 K for 1 h with a ramping rate of 10 K/min. After the reduction, a 10 mL/min of pure NH_3 (99.999%) was used for measured. The expected reaction temperature (for instance to 623 K) was achieved by using a ramping rate of 5 K/min. In all experiments, the catalytic NH_3 decomposition performance was investigated under steady temperature state. Both, the reactant and products were analyzed by using GC instrument (SC-200, China) provided with a Poropak Q column and thermal conductivity detector with Ar as carrier gas.

The conversion of NH_3 (X_{NH_3}) was calculated by using the following equation:

$$X_{NH_3} = \frac{(A_{NH_3,in} - A_{NH_3,out})}{A_{NH_3,in}} \times 100\%$$

Where $A_{NH_3,in}$ = Amount of ammonia in feed;

$A_{NH_3,out}$ = Unconverted amount of ammonia.

2. TEM images of supported Ni/MCF-17 catalysts

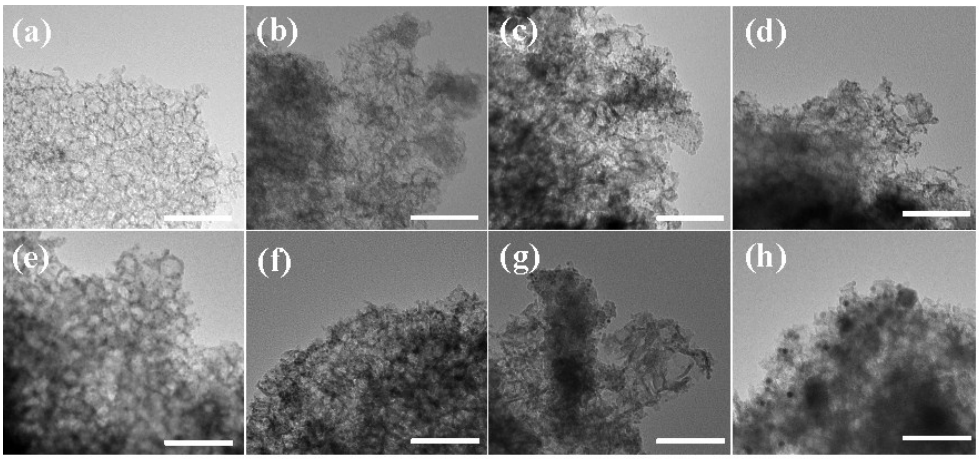

Fig. S1. TEM images of Ni/MCF-17 catalysts composed of different particle size nanocrystals of (a) 0.06NiR180/MCF-17, (b) NiR180/MCF-17, (c) NiR150/MCF-17, (d) NiR110/MCF-17, (e) NiR90/MCF-17, (f) NiCR90/MCF-17, (g) NiCR110/MCF-17 and (h) Ni180/MCF-17. The scale bar is 100 nm.

3. BET patterns of supported Ni/MCF-17 catalysts

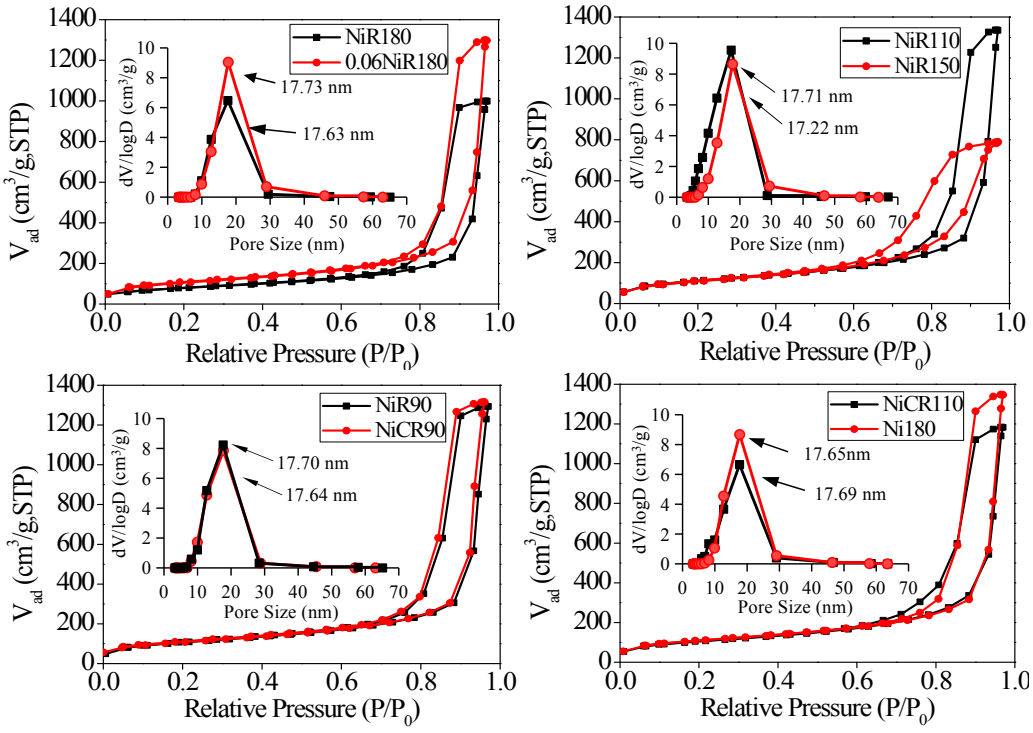

Fig. S2. The N_2 adsorption-desorption isotherms and corresponding BJH mesopore size distribution curves measured at 77 K after degassing the samples for 3 h at 573 K.

Table S1 Comparison of Ni loadings, textural properties, particle sizes and catalytic performances of Ni/MCF-17 catalysts (catalytic performance measured at 575 °C, pure NH_3, GHSV = 6000 $mL g_{cat}^{-1} h^{-1}$ and 0.1 MPa)

Catalysts	Ni loadings[a] (wt %)	Surface areas ($m^2 g^{-1}$)	Pore sizes (nm)	Pore volumes ($cm^3 g^{-1}$)	Ni dispersion (%)	Ni particle size (nm)			Activity (CTY) [b]	HTOF [c]
						By TEM	By XPS	By H_2 chemisorption		
MCF-17	–	573.16	17.05	2.32	–	–	–	–	–	–
0.06NiR180	0.90	509.37	17.73	2.11	41.94	1.5	16.0	1.36	1.91	28.3
NiR180	0.73	532.21	17.63	1.66	34.22	1.8	18.9	2.46	2.20	25.0
NiR150	0.40	526.11	17.22	1.98	10.85	2.5	23.2	7.78	2.71	50.5
NiR110	0.56	561.20	17.71	2.13	49.74	3.0	15.3	2.04	2.75	56.1
NiR90	0.74	546.33	17.70	2.18	57.60	3.4	18.2	1.76	2.54	22.2
NiCR90	0.64	570.12	17.64	2.17	61.86	4.0	15.7	1.64	2.70	33.7
NiCR110	0.67	542.97	17.65	1.93	18.82	4.5	17.1	4.48	2.62	29.4
Ni180	0.72	557.76	17.69	2.21	41.75	8.0	19.8	11.75	1.22	12.5

[a] The values obtained from ICP. [b] CTY: 10^{-3} $mol_{NH_3} \cdot g_{Ni}^{-1} \cdot s^{-1}$.

[c] HTOF: 10^{-3} s^{-1} based on Ni dispersion from H_2 chemisorption.

4. XRD analysis of the reduced Ni/MCF-17 catalysts

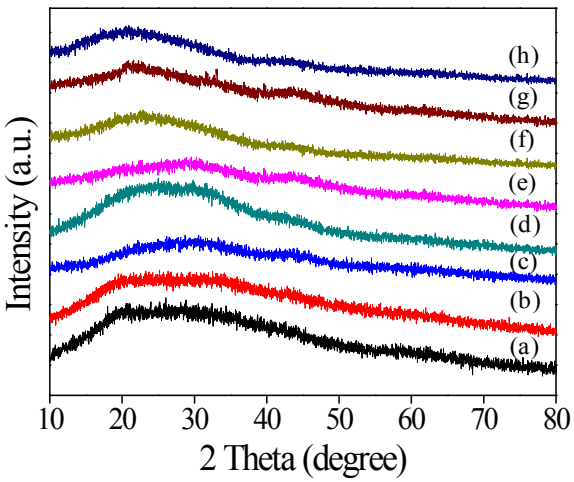

Fig. S3. XRD patterns of the reduced Ni/MCF-17 catalysts of (a) 0.06NiR180, (b) NiR180, (c) NiR150, (d) NiR110, (e) NiR90, (f) NiCR90, (g) NiCR110 and (h) Ni180. The catalysts were reduced in a 5% H_2/Ar mixture gas flow at 673 K for 3 h.

To identify the possible impact of Ni precursor quantities and reduction temperature on the phase composition, all the as-prepared catalyst were characterized by using XRD studies and results are shown in Fig. S3. Almost, all the XRD patterns are

identical and exhibited uniform crystalline structure, with only one obvious characteristic peak in the range of 21° to 25°, attributed as the Ni (1 0 1) plane. An indication that the reduced Ni-base catalysts are still relatively composed of pure Ni phase. In addition, an increase in the peak intensity is consistent with a higher Ni loading. The samples who posses narrower full width at half maximum (FWHM) of the diffraction peaks,[1] indicated larger particles and it agrees to the TEM observations.

5. XPS analysis of the Ni_{2p} in Ni/MCF-17 catalysts

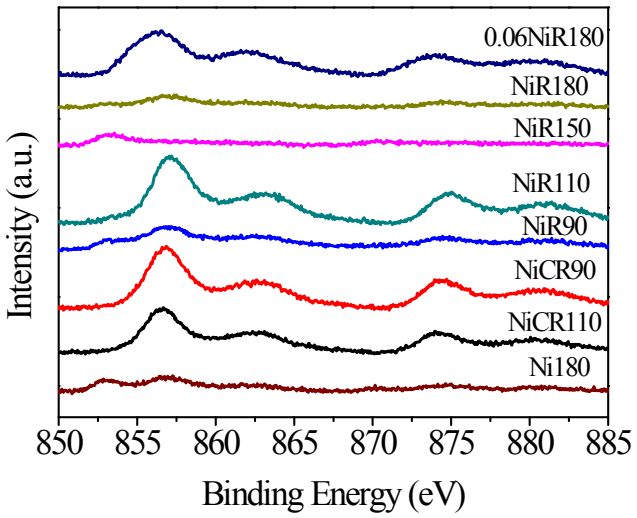

Fig. S4. XPS patterns of the Ni_{2p} in Ni/MCF-17 catalysts.

To probe the surface properties of Ni/MCF-17 catalysts, the Ni_{2p} XPS patterns was used and obtained results are shown in Fig. S4. Based on the published data,[2, 3] the major nickel phase could be inferred from following binding energies:

i.NiO intimately interacting with support is around 856.0 eV) and

ii.Bulk NiO is around 854.0 eV.

The detected $Ni_{2p3/2}$ levels is shifted from 853.29 eV (in NiR150/MCF-17) to 857.16 eV (in NiR110/MCF-17). The binding energies of the Ni-based catalysts show one major peak around 856.0 eV except NiR150/MCF-17. A vivid indication that that Ni exists in NiO form in all the Ni-based catalysts and NiO intimately interacts with support. In addition, the NiO peaks at the binding energy of 853.29 eV (in case of NiR150/MCF-17) is attributed to formation bulk NiO species.

Table S2 Summary of major Ni phase, Ni_{2p} binding energy and atomic ratio of Ni-based catalysts determined by XPS analysis.

Catalysts	Major Ni phase	Ni_{2p} binding energy, eV	Atomic ratio n_{Ni}/n_{Si} (*10^{-3})	Atomic ratio n_{Ni}/n (*10^{-3})
0.06NiR180	NiO	856.33	10.33	0.09
NiR180	NiO	857	3.97	0.20
NiR150	NiO	853.29	1.94	0.34
NiR110	NiO	857.16	13.20	0.07
NiR90	NiO	857.01	5.31	0.19
NiCR90	NiO	856.83	11.42	0.09
NiCR110	NiO	856.62	7.68	0.12
Ni180	NiO	856.86	2.69	0.27

Summary of the major Ni phase, Ni_{2p} binding energy and relative atomic ratio of Ni:Si and relative content of Ni in Ni/MCF-17 catalysts determined by XPS analysis is shown in Table S2. The highest atomic ratio of n_{Ni}:n_{Si} ≈ 13.20×10^{-3} in NiR110/MCF-17 which is approximately 7 times higher than of lowest atomic ratio of Ni:Si in NiR150/MCF-17 (≈1.94×10^{-3}). Whereas the atomic ration $n_{Ni}/n = 11.66\times10^{-3}$ and 1.90×10^{-3} for NiR110/MCF-17 and NiR150/MCF-17 catalyst, respectively. According to previous publication,[4] the sizes of Ni particles obtained from the intensity of XPS signal by using Kerkhof-Moulijn method measured at different relative atomic concentrations $(n_{Ni}/n_{Si})_{exp}$. Lower relative intensity of Ni_{2p} XPS experimental signal $(n_{Ni}/n_{Si})_{exp}$ indicates large Ni particles. This could be because of considerable number of Ni atoms located in the bulk of Ni particles where they may not be detectable by XPS. As the catalyst NiR150/MCF-17 yielded the lowest $(n_{Ni}/n_{Si})_{exp}$, an indication of largest Ni particle size in the nickel-based catalysts. In fact, the order of particles size by XPS studies are NiR110/MCF-17 < NiCR90/MCF-17 < 0.06NiR180/MCF-17 ≈ NiCR110/MCF-17 NiR90/MCF-17 < NiR180/MCF-17 ≈ Ni180/MCF-17 < NiR150/MCF-17.

6. TEM images of reduced Ni/MCF-17 catalysts

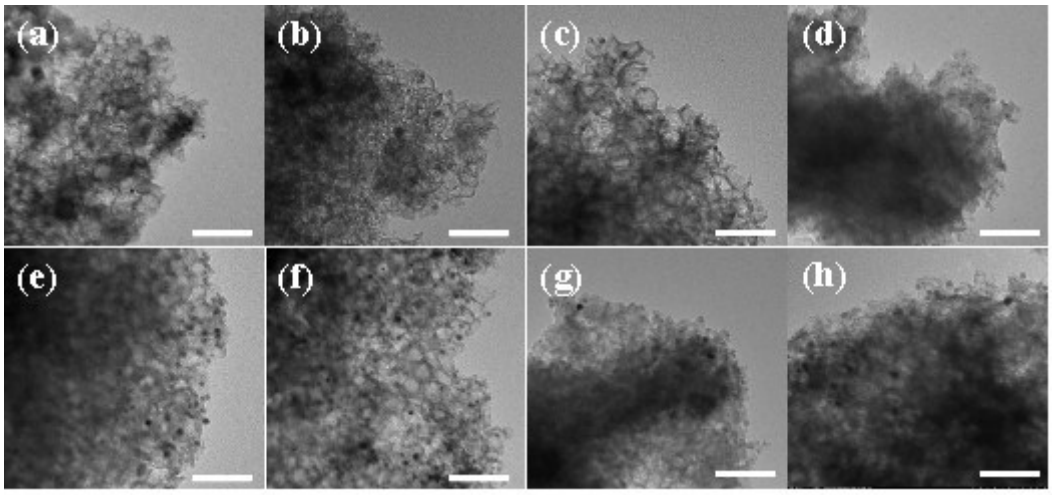

Fig. S5. The TEM images of reduced Ni/MCF-17 catalysts of (a) 0.06NiR180/MCF-17, (b) NiR180/MCF-17, (c) NiR150/MCF-17, (d) NiR110/MCF-17, (e) NiR90/MCF-17, (f) NiCR90/MCF-17, (g) NiCR110/MCF-17 and (h) Ni180/MCF-17. The catalysts were reduced in a 5% H_2/Ar mixture gas flow at 673 K for 3 h. The scale bar is 100 nm.

7. NH_3 decomposition stability test of NiR110/MCF-17 catalyst

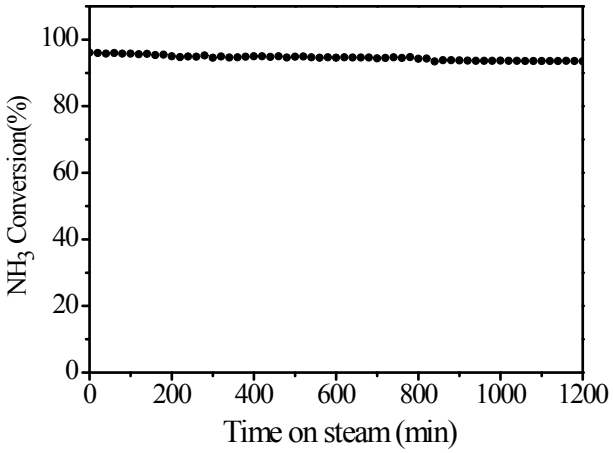

Fig. S6. NH_3 decomposition stability test of NiR110/MCF-17 catalyst (Reaction conditions: Pure NH_3, GHSV = 6000 $mL \cdot g_{cat}^{-1} \cdot h^{-1}$, 0.1 MPa and 20 h).

8. HAADF-STEM and EDX mapping of NiR110/MCF-17 catalyst

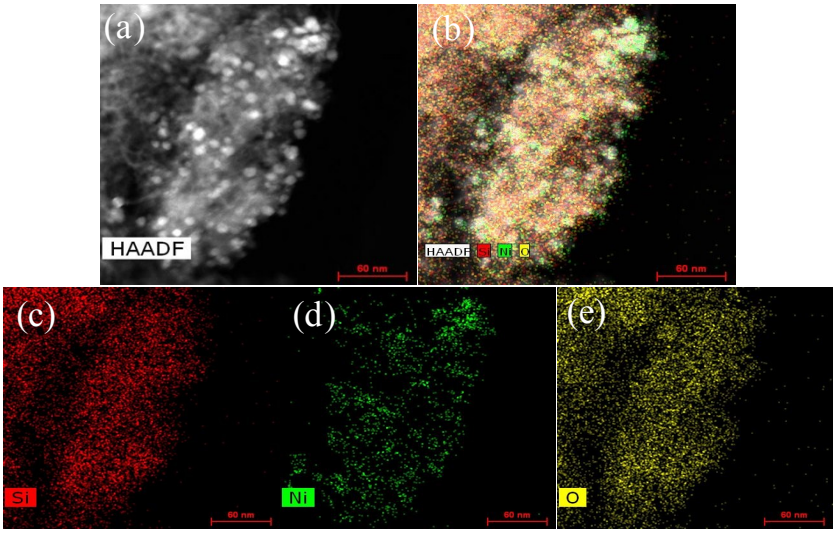

Fig. S7. (a) HAADF-STEM image of NiR110/MCF-17 catalyst and EDX mapping spectra of (b) all element, (c) Si, (d) Ni and (e) O . The scale bar is 60 nm.

9. Establishment of basic cubo-octahedron structure model and relationship between the concentration of B_5 sites and average Ni particles size

According to results published by Hardeveld *et al.*[5], a basic cubo-octahedron structure model was established and a better approximation to a spherical shape can obtained. This model assumes that cubo-octahedron is symmetrical and the cube planes and the octahedron planes have the same size. If there are *n* atoms arranged along the edge of the cube plane and *m* atoms located along the intersection line of octahedron planes, the octahedron plane was composed of alternating non-regular hexagons with m and n atoms along the edges, and the cube planes are square. Therefore, the concentration of B_5 sites can be calculated according to eqs. (S1) ~ (S4), among, the basic atoms of number N_{basic} of cubo-octahedron is

$$N_{basic} = \frac{1}{3}(m+2n-2)\{2(m+2n-2)^2+1\} - n(n-1)(2n-1) \qquad (S1)$$

Additional atoms were place as incomplete layers, the maximum B_5 sites number

$n(B_5)_{max}$ is

$$n(B5)_{max} = 8\{3[(m-3)+(n-2)]\}+6[4(n-3)] = 24(m+2n-8) \qquad (S2)$$

The atoms number of added in incomplete layer N_{ad} (with condition $m > 3$ and $n > 2$) is

$$N_{ad} = 8\{\frac{1}{2}[(m-2)+2(n-2)][(m-2)+2(n-2)+1] - 3[\frac{1}{2}(n-2)(n-1)]\}+6(n-3)^2 \qquad (S3)$$

The total atoms number of which make up cubo-octahedron structure model N_{total} is

$$N_{total}=N_{basic}+N_{ad} \qquad (S4)$$

According to the above formula, take $m = n$, a series of numbers were calculated for this model are shown in Table S3.

Table S3 The a series of numbers N_{basic}, N_{ad}, N_{total} and $n(B_5)_{max}$ of basic cubo-octahedron structure model.

m	N_{basic}	N_{ad}	N_{total}	$n(B_5)_{max}$	B_5 sites concentration [a]	$d_{(Ni)}$, Å
3	201	24	225	24	0.107	16.8
4	586	102	688	96	0.140	24.4
5	1289	240	1529	168	0.110	31.8
6	2406	438	2844	240	0.084	39.1
7	4033	696	4729	312	0.066	46.5
8	6226	1014	7240	384	0.053	53.8
9	9201	1392	10593	456	0.043	61.0
10	12934	1830	14764	528	0.036	68.1

Here, $d_{(Ni)} = \sqrt[3]{\frac{6(\sqrt{2}d_{at})^3}{4\pi}N_{total}} = 1.11\sqrt[3]{N_{total}}d_{at}$; d_{at}(Ni)=2.49 Å ;

B_5 sites concentration $= \frac{n(B_5)_{max}}{N_{total}}$.

According to the data of Column 6 and Column 7 in Table S3, the relationship curve

between the concentration of B_5 sites and average Ni particles size can be ploted.

10. References

1. C. Zhang, S. Hwang and Z. Peng, *J. Mater. Chem. A*, 2014, **2**, 19778–19787.
2. Y. J. Huang, J. A. Schwarz, J. R. Diehl and J. P. Baltrus, *Appl. Catal.*, 1988, **36**, 163–175.
3. P. Legare and A. Fritsch, *Surf. Interface Anal.*, 2010, **15**, 698–700.
4. A. Y. Khodakov, A. Griboval-Constant, R. Bechara and V. L. Zholobenko, *J. Catal.*, 2002, **206**, 230–241.
5. R. V. Hardeveld and A. V. Montfoort, *Surf. Sci.*, 1966, **4**, 396-430.